Electronic Supplementary Material (ESI) for CrystEngComm.

Supplementary information

Enhancement of Photocatalytic Performance in Two Zinc-Based Metal-Organic Frameworks by Solvent Assisted Linker Exchange

Mohammad Yaser Masoomi,‡ Minoo Bagheri‡ and Ali Morsali*

Department of Chemistry, Faculty of Sciences, TarbiatModares University, P.O. Box 14115-175, Tehran, Islamic Republic of Iran

Email: Morsali_a@modares.ac.ir, Morsali_a@yahoo.com

‡ These authors contributed equally to this work.

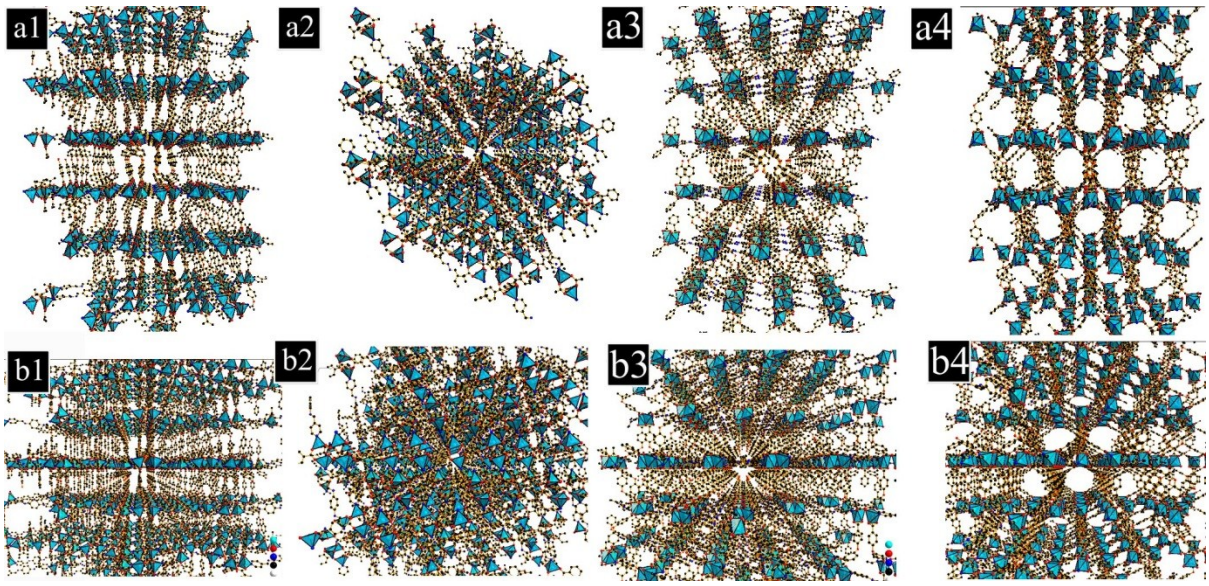

Fig. S1. (a1-a4) Ball and stick representation of TMU-4 along the *a*-, *b*-, *c*-axes and [1 0 1] direction. (b1-b4) Ball and stick representation of TMU-6 along the *a*-, *b*-, *c*-axes and [1 0 1] direction. Color code: O: red; N: blue; C: black; and Zn: blue polyhedra. DMF molecules are omitted for clarity.

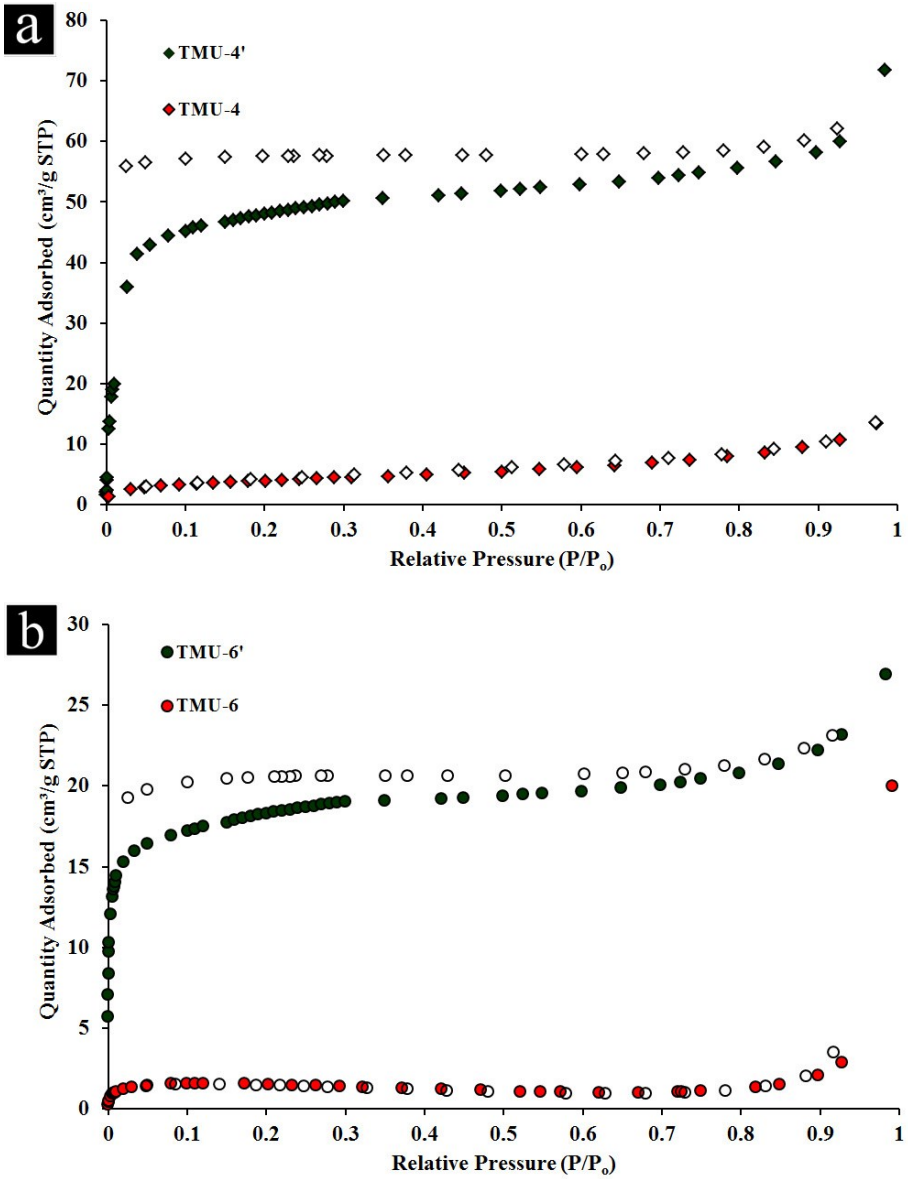

Fig. S2. N_2 isotherms collected at 77 K and 1 bar on (a) TMU-4 and TMU-4' and (b) TMU-6 and TMU-6'.

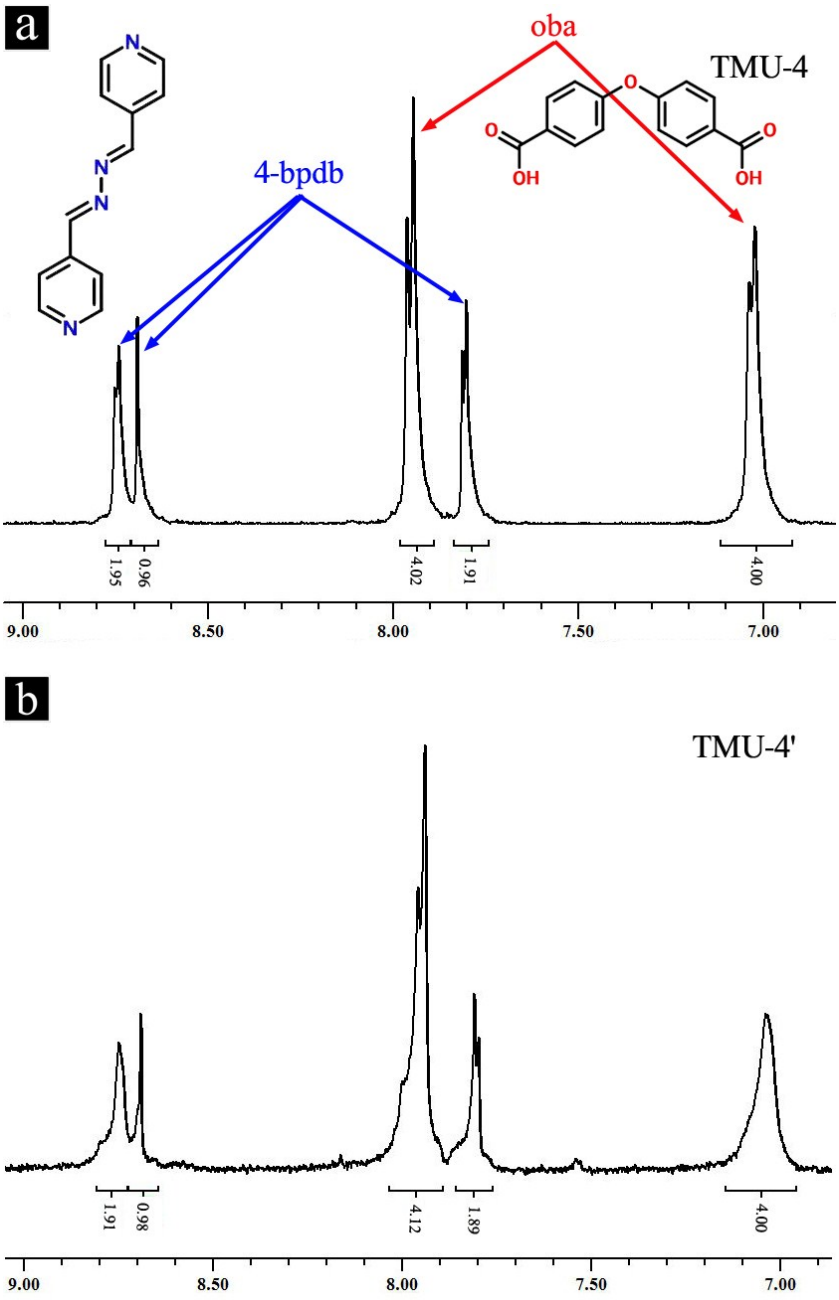

Fig. S3. The ^{1}H NMR spectra of (a) the digested sample of TMU-4 and (b) the linker-exchange process in TMU-6 with 4-bpdb after 21 days (100% exchange) (D_2SO_4/d_6-DMSO).

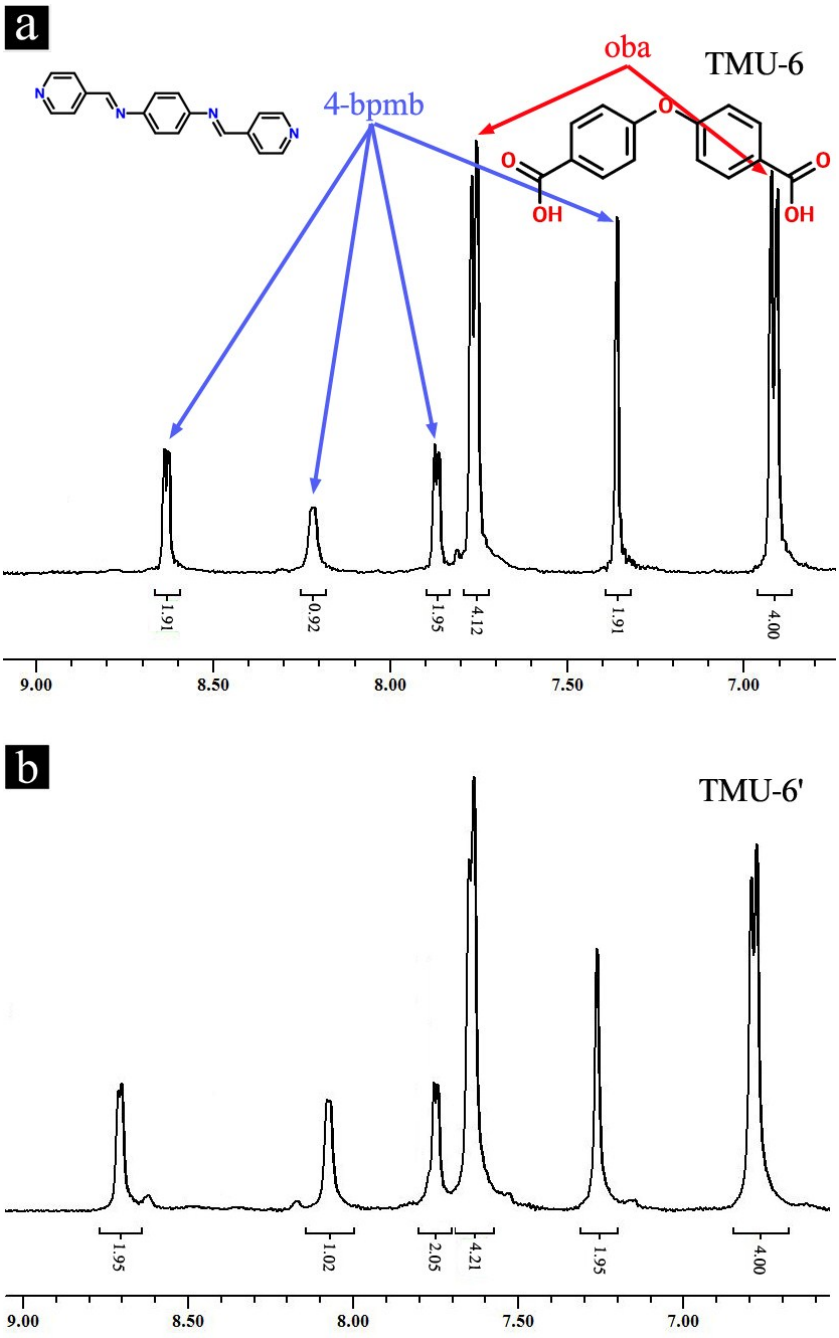

Fig. S4. The ^{1}H NMR spectra of (a) the digested sample of TMU-6 and (b) the linker-exchange process in TMU-4 with 4-bpmb after 24 h (100% exchange) (D_2SO_4/d_6-DMSO).

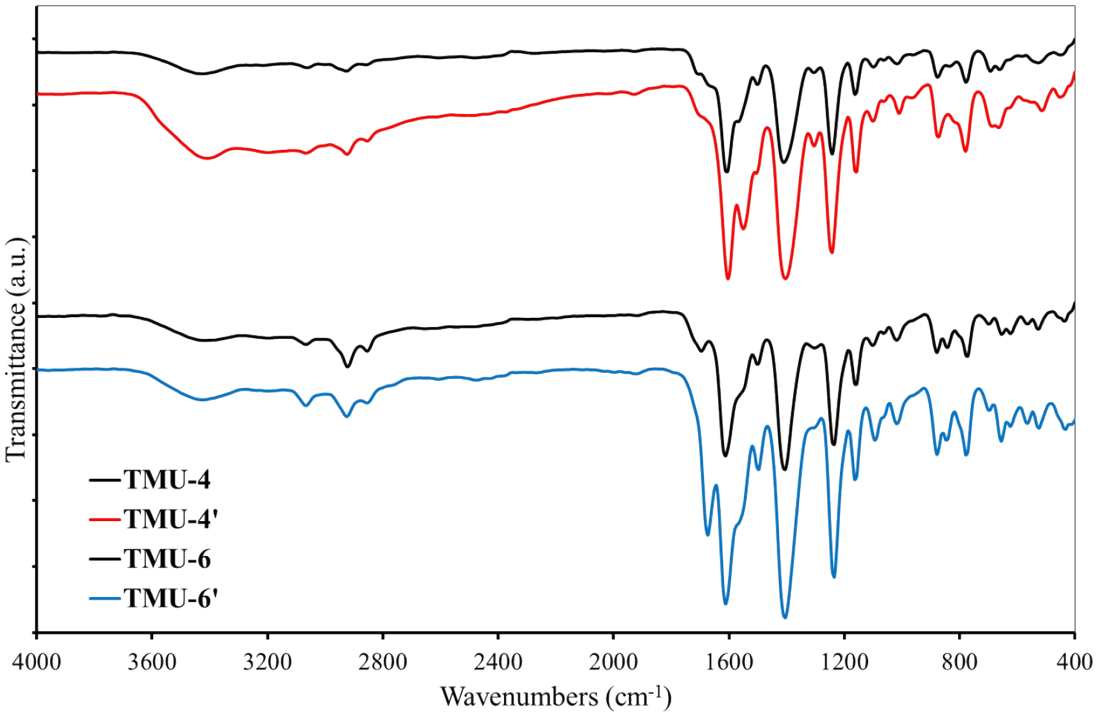

Fig. S5. IR spectra of parent TMU-4 and TMU-6 and daughter TMU-4' and TMU-6' after SALE peocess.

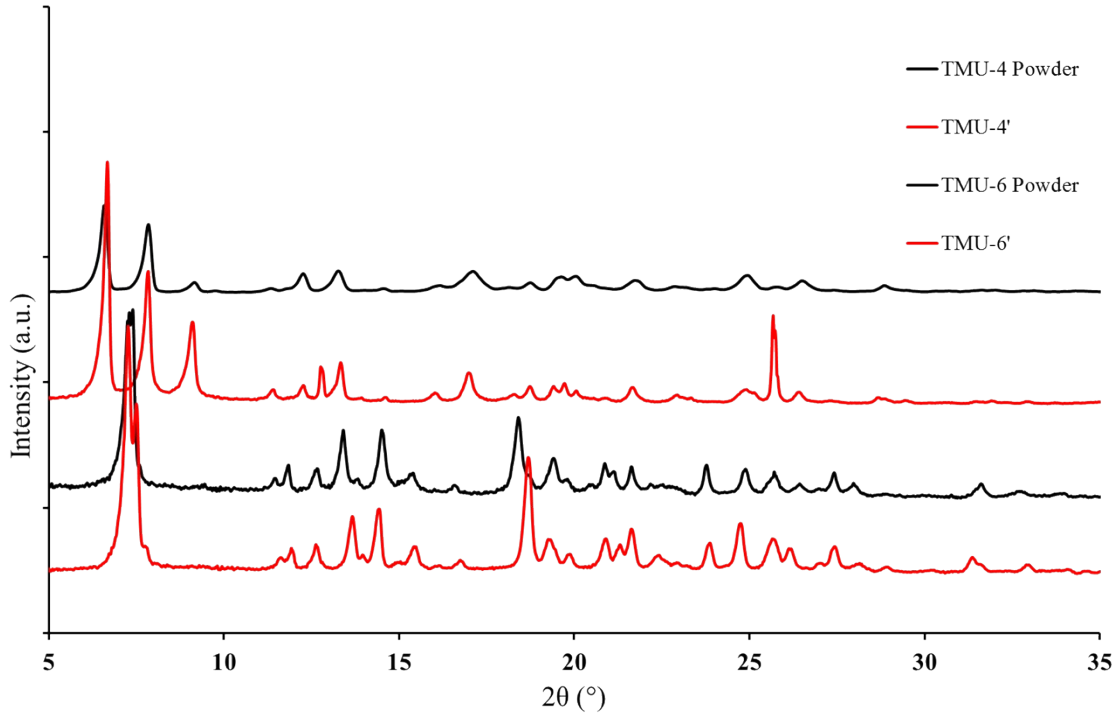

Fig. S6. Comparison of XRD patterns for parent TMU-4 and TMU-6 and their daughter synthesized via SALE.

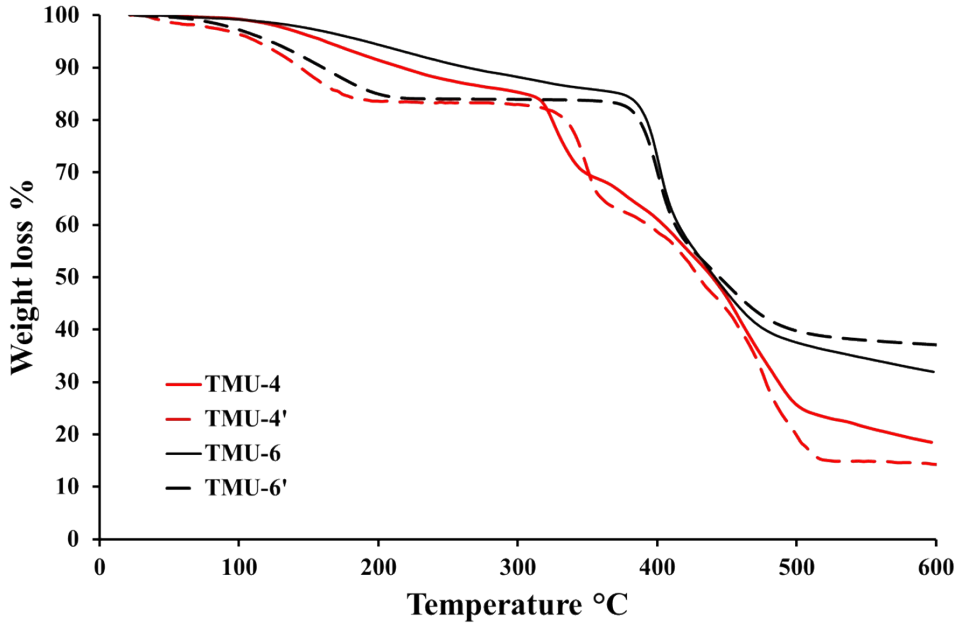

Fig. S7. Thermogravimetric profiles of TMU-4, TMU-4', TMU-6 and TMU-6'.

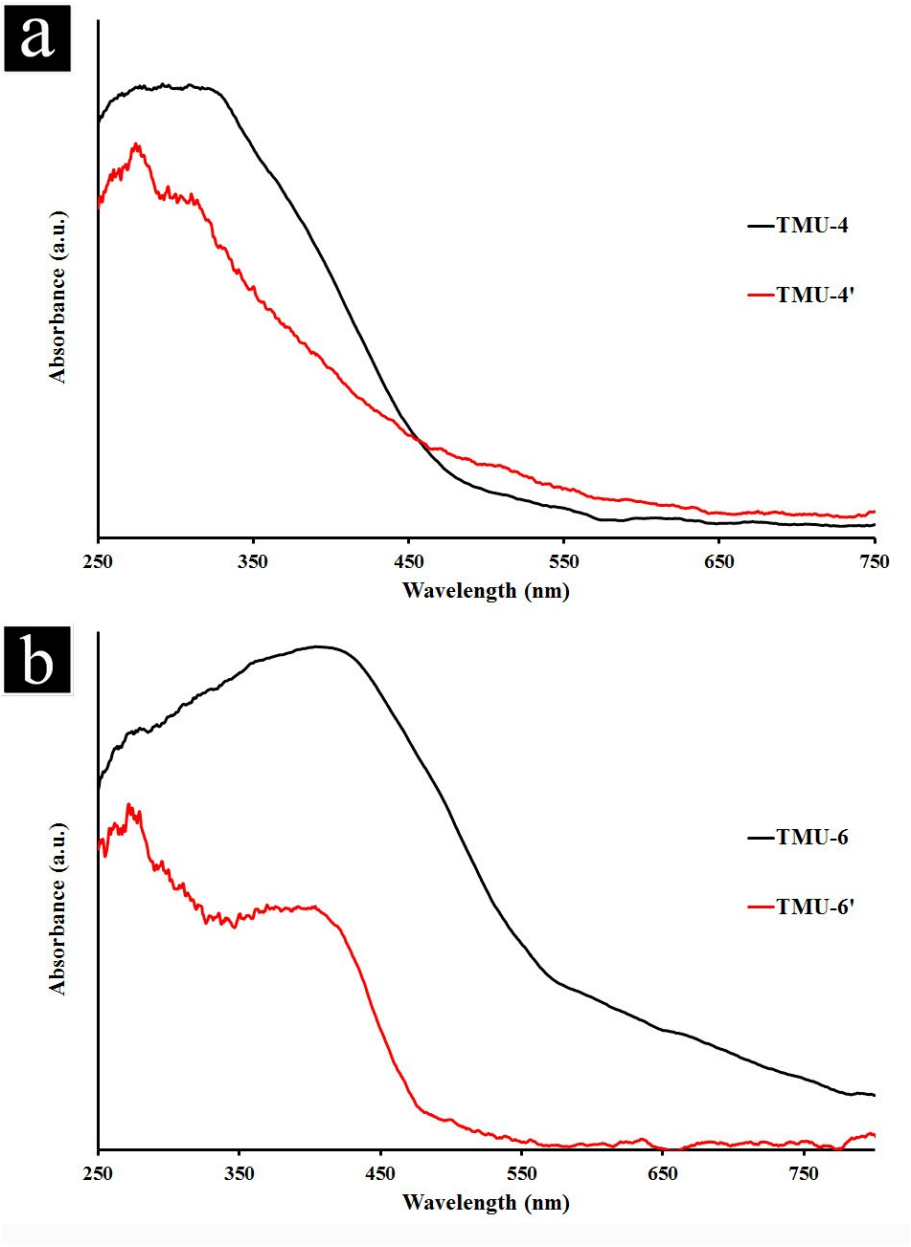

Fig. S8. UV-vis diffuse reflectance spectra of the MOFs.

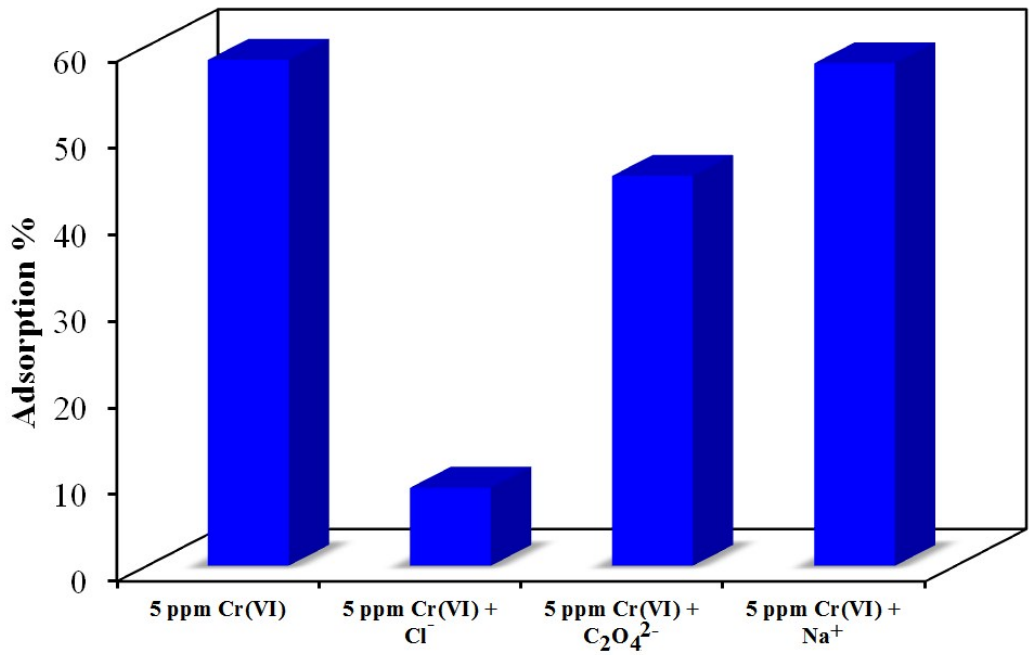

Fig. S9. Effect of different ions on adsorption of 5 ppm Cr(VI) in presence of TMU-4' as the best adsorbent.

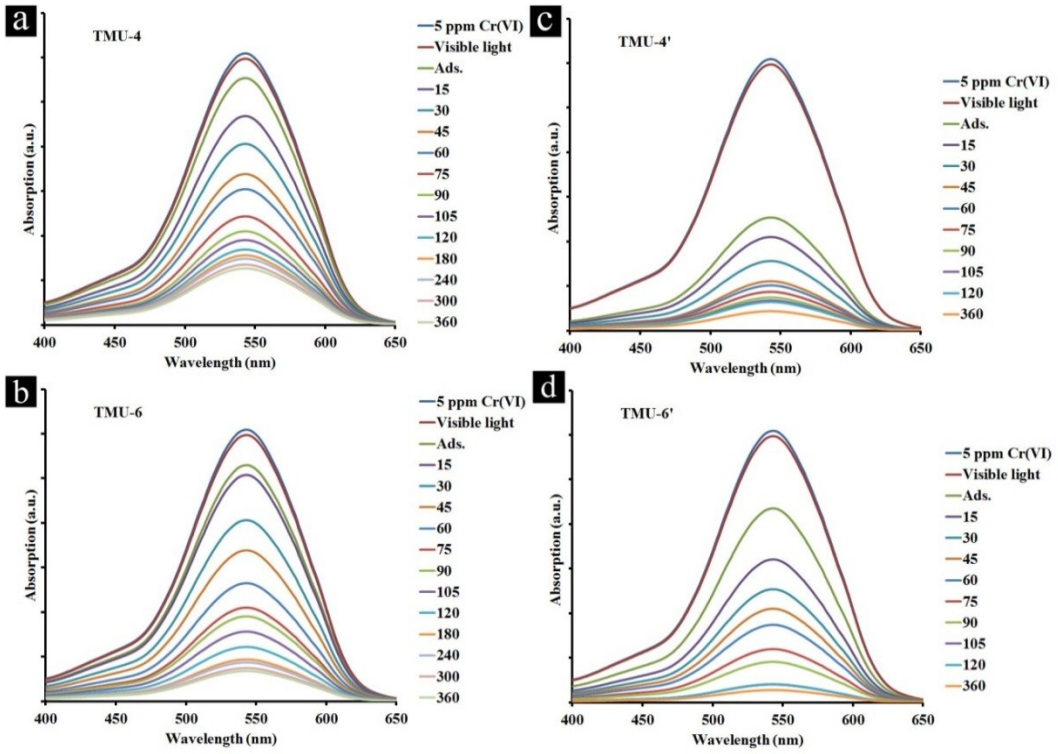

Fig. S10. UV-vis spectra of DPC solution in presence of Zn-based MOF photocatalysts under visible light.

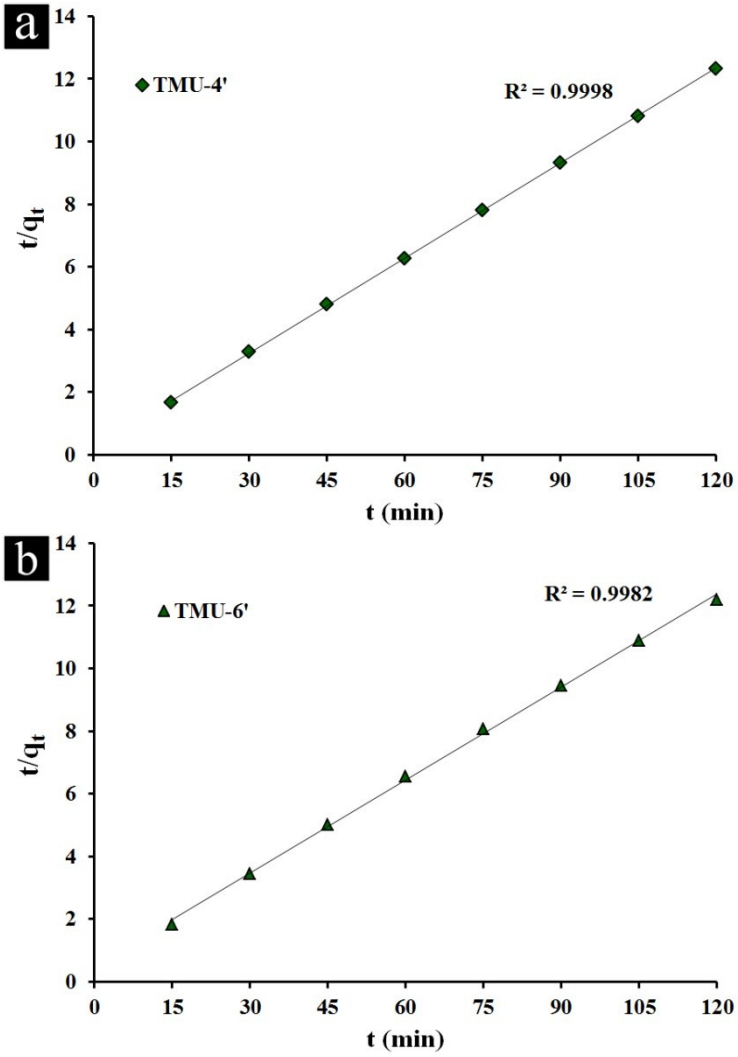

Fig. S11. Effect of time on Cr(VI) reduction described by pseudo-second order linear plots over a) TMU-4' and b) TMU-6' MOFs.

Table S1. BET surface area and adsorption properties of Zn-based MOFs in presence of various concentrations of Cr(VI) solution for 1 h.

MOFs	Adsorption (%)				BET (m^2/g)
	5 ppm	10 ppm	15 ppm	20 ppm	
TMU-4	9.2	5.4	2.5	1.8	1
TMU-6	9.1	4.9	2	1.2	6
TMU-4'	58.4	45.6	32.7	23.8	207
TMU-6'	30.3	25.7	19.5	12.3	68